Autonomous Helicopter Control Using Gradient Descent Optimization Method

B. Kadmiry
Dept. of Computer Sci.
Linköping University
581 83 Linköping, Sweden
bouka@ida.liu.se

R. Palm
Dept. ZK IK 4
Siemens AG Corporate Technology
81739 Munich, Germany
rainer.palm@mchp.siemens.de

D. Driankov
Dept. of Computer Sci.
Linköping University
581 83 Linköping, Sweden
ddr@ida.liu.se

Abstract

The work reported in this paper is aimed at designing a velocity/altitude and position controllers for the unmanned helicopter APID MK-III by Scandicraft AB in Sweden. The controllers are able of regulating high velocities via stabilization of the attitude angles within much larger ranges than currently available. We use a novel approach to the design consisting of two steps: first, a gradient descent optimization method is used to compute for each desired horizontal velocity/altitude or position the corresponding desired values for the attitude angles and the main rotor collective pitch; second, a linear control scheme is used to regulate the attitude angles so that the helicopter achieves its desired horizontal velocity at the desired altitude, or its desired position. The performance of the controllers is evaluated in simulation and shows that the proposed design method achieves its intended purpose.

1 Introduction

The overall objective of the Wallenberg Laboratory for Information Technology and Autonomous Systems (WITAS) at Linköping University is the development of an intelligent command and control system, containing active-vision sensors, which supports the operation of a unmanned air vehicle (UAV) in both semi- and full-autonomy modes. One of the UAV platforms of choice is the APID MK-III unmanned helicopter, by Scandicraft Systems AB (www.scandicraft.se). The intended operational environment is over widely varying geographical terrain with traffic networks and vehicle interaction of variable complexity, speed, and density. The present version of APID MK-III is capable of autonomous take-off, landing, and hovering as well as of autonomously executing pre-defined, point-to-point flight where the latter is executed at low-speed. This is enough for performing missions like site mapping and surveillance, and communications, but for the above mentioned operational environment much higher speed is desired. In this context, our goal is to explore the possibilities for achieving high-speed motion through stable "aggressive" manoeuvrability at the level of attitude control (pitch, roll, and yaw) and test a variety of control solutions in the APID MK-III simulation environment (see [3]).

In this work we present a novel design method for velocity/altitude and position controllers based on a two-step synthesis using a mathematical model of APID MK-III. The controllers achieve stabilization within much larger ranges for the attitude angles and horizontal velocities than currently available and their performance is evaluated in simulation. The two-step synthesis proceeds as follows:

1. given desired horizontal velocities and altitude or a position, a gradient descent optimization method, applied to the equations of motion (translational motion) computes desired values for attitude angles and the main rotor collective pitch (main collective). Having a particular value for the latter transforms the nonlinear-in-the-input attitude (angular motion) equations into a system of linear equations where the control inputs are decoupled.

2. on the basis of the decoupled linear attitude equations and the desired values for the attitude angles, stabilizing linear control laws for the tail collective pitch, longitudinal and lateral cyclics are designed.

The approach, as shown in simulation, shows to be an effective control strategy enabling a high-speed horizontal motion (in the range of $[-36, 100]$ km/h for backward/forward motion and $[-36, 36]$ km/h for sideward motion) and altitude stabilization. The ranges for the attitude angles that allow us to achieve this are within the intervals $-\pi/4 \leq \phi \leq \pi/4, -\pi/4 \leq \theta \leq \pi/4, -\pi \leq \psi \leq \pi$.

In Sect. 2 we introduce the model of APID MK-III used for velocity/altitude and position control and the basic underlying assumptions used in its derivation. We also point out the differences between this model and the ones used by the Berkeley AeRobot team (BEAR) and the Georgia Tech ASRT system. In Sect. 3 we present the synthesis approach and apply it to the design and analysis of the velocity/altitude controller. Furthermore in Sect. 3.1 we introduce the position controller. In Sect. 4 we provide results from simulation that illustrate the performance of the proposed controllers. Section 5 presents conclusions and directions for future work.

2 The APID MK-III Model

The mathematical model used for control of APID MK-III is of the form:

$$\ddot{x} = \frac{1}{m}(F_N - k\omega^2\theta_0(c\phi s\theta c\psi + s\phi s\psi)), \quad (1)$$

$$\ddot{y} = \frac{1}{m}(F_E - k\omega^2\theta_0(c\phi s\theta s\psi - s\phi c\psi)), \quad (2)$$

$$\ddot{z} = \frac{1}{m}(F_D + F_g - k\omega^2\theta_0 c\phi c\theta), \quad (3)$$

$$\ddot{\phi} = -a\dot{\phi} + dk\omega^2\phi_c\theta_0, \quad (4)$$

$$\ddot{\theta} = -b\dot{\theta} - ek\omega^2\theta_c\theta_0, \quad (5)$$

$$\ddot{\psi} = -c\dot{\psi} + f(\alpha_{tr} - \psi_0), \quad (6)$$

where $c\phi = cos\phi$ and $s\phi = sin\phi$. The state vector is $(x, y, z, \phi, \theta, \psi, \dot{x}, \dot{y}, \dot{z}, \dot{\phi}, \dot{\theta}, \dot{\psi})$, i.e., positions, attitude angles, and their respective velocities. The control inputs are $(\phi_c, \theta_c, \theta_0, \alpha_{tr})$, i.e., these are the usual controls in terms of lateral and longitudinal cyclic pitches, and collective pitches for the main and tail rotors. The first three equations describe the dynamics of translational motion in the inertial frame where $F_\circ$ are wind forces in north, east, and vertical directions; m is the helicopter body mass, F_g is the gravity force acting on the cabin, and ω is the main rotor RPM. The last three equations describe the dynamics of the rotational motion in the body frame. The coeficients $a = 38.7072$, $b = 10.1815$, $c = 0.434$ are derived from the expression of moment equations leading to the attitude angles' equations ($\psi_0 = 0.09$ is an offset term).

The assumptions underlying the above model are: (i) the variation of the rotor speed ω is constant as a consequence of maintaining constant throttle control at the nominal part of the power curve – the constant value of ω is implicit in the gain $k\omega^2 = 1703.46$, and (ii) the variations of the main rotor angles are small enough so that the magnitude of the main rotor force can be considered equal to the thrust force.

The uncertainty or unmodeled dynamics of the above model can be categorized as follows: (i) unmodeled aerodynamics – only the wind action, e.g.,

F_N, F_E, F_D on the body is considered, and the action of the tail rotor force on the angular acceleration (pitch) is neglected; (ii) higher order dynamics such as rotor flapping dynamics is not considered at all, while the usually highly nonlinear link between the control inputs and servos of the main and tail rotors and governing equations are linearized and are implicit in the constant gains $k\omega^2 = 1703.4$, $dk\omega^2 = 223.5824$, $ek\omega^2 = 58.3258$, and $f = 31.9065$; and (iii) servo actuators are linked to the control inputs and are modeled by first-order transfer functions of the form $\dot{\delta} = -300\delta + 300u$ where u is any one of the control inputs and δ is a pseudo state variable.

The current control system for APID MK-III does not utilize large ranges of the rotor attitude angles. As a consequence this produces lower rate-of-change of the attitude angles ϕ, θ and ψ, and consequently the control is done on rather small ranges for these – all this reduces manoeuvrability w.r.t. these angles and consequently the speed of motion. In this context, the objective of our study is to design a velocity/position controller which acts on much larger ranges of the attitude angles, i.e., $-\pi/4 \leq \phi \leq +\pi/4$, $-\pi/4 \leq \theta \leq +\pi/4$, $-\pi \leq \psi \leq +\pi$, by utilizing the full range of the rotor attitude angles. The latter, for the purpose of this study, are in the interval $[-0.7, +0.7]$ rad.

As already mentioned above, the contribution of the tail rotor force and the tail rotor torque are not reflected in Eqs. (2) and (4), while in the BEAR model [1] this contribution is accounted for. With regard to the Georgia Tech ASRT model [2] the difference is that, their dynamic inversion control is based on dynamics linearized about a nominal operating point. Then a direct NN based adaptive control architecture is used to adapt to errors caused by the linearized inverted model. In our work the velocity/altitude controller is designed using the original nonlinear model without linearizing it.

3 Velocity/Altitude Controller

The equations of motion of the helicopter can be represented by two levels. The equations at the upper level describe the dynamic behavior of the system in absolute coordinates (x, y, z):

$$\ddot{x} = \frac{1}{m}(F_N - k\omega^2\theta_0(c\phi s\theta c\psi + s\phi s\psi)),$$

$$\ddot{y} = \frac{1}{m}(F_E - k\omega^2\theta_0(c\phi s\theta s\psi - s\phi c\psi)), \quad (7)$$

$$\ddot{z} = \frac{1}{m}(F_D + F_g - k\omega^2\theta_0 c\phi c\theta),$$

where the angles (ϕ, θ, ψ) and the angle θ_0 act as control inputs. The equations at the lower level describe the dynamic behavior of the attitude angles (ϕ, θ, ψ):

$$\ddot{\phi} = -a\dot{\phi} + dk\omega^2\theta_0\phi_c,$$
$$\ddot{\theta} = -b\dot{\theta} - ek\omega^2\theta_0\theta_c, \qquad (8)$$
$$\ddot{\psi} = -c\dot{\psi} + f(\alpha_{tr} - \psi_0),$$

where θ_0 is given by the upper level, $(\phi_c, \theta_c, \alpha_{tr})$ acts as control input vector, θ_0 is an angle connected to the trust force, and k, a, b, c, d, e, f are given positive constants.

The control problem for the upper level is to calculate angles (ϕ, θ, ψ) and θ_0 so that given velocities $(\dot{x}_d, \dot{y}_d)$ and a given position (altitude) z_d are reached in a certain amount of time. This requires specific angles $(\phi_d, \theta_d, \psi_d)$ and a corresponding thrust force angle θ_0. The control problem for the lower level is to adjust the angles $(\phi_d, \theta_d, \psi_d)$ calculated by the upper level. The control law design for the lower level is straight-forward. We require the lower level to follow a be-havior that is determined by three decoupled second order linear equations:

$$\ddot{\phi} = k_{\dot{\phi}}\dot{\phi} + k_{\phi}(\phi - \phi_d),$$
$$\ddot{\theta} = k_{\dot{\theta}}\dot{\theta} + k_{\theta}(\theta - \theta_d), \qquad (9)$$
$$\ddot{\psi} = k_{\dot{\psi}}\dot{\psi} + k_{\psi}(\psi - \psi_d).$$

The corresponding gains $k_{\dot{\phi}}$, $k_{\dot{\theta}}$, and $k_{\dot{\psi}}$ are designed in a classical way by a robust pole placement or other appropriate methods. Comparing the right-hand sides (RHS) of (8) and (9) the corresponding control inputs are calculated as:

$$\phi_c = \frac{1}{dk\omega^2\theta_0}(\dot{\phi}(k_{\dot{\phi}} + a) + k_{\phi}(\phi - \phi_d)),$$
$$\theta_c = \frac{-1}{ek\omega^2\theta_0}(\dot{\theta}(k_{\dot{\theta}} + b) + k_{\theta}(\theta - \theta_d)), \quad (10)$$
$$\alpha_{tr} = \frac{1}{f}(\dot{\psi}(k_{\dot{\psi}} + c) + k_{\psi}(\psi - \psi_d)) + \psi_0.$$

In contrast to the lower level, the upper level control problem cannot be solved in a straightforward man-ner because of: (i) the nonlinearities in the RHSs of (7), and (ii) the fact that the system is over-determined which means that there are more control inputs than outputs. The first design step is, similar to the lower level, to require a predefined behavior of the system in external coordinates, that is,

$$\ddot{x} = k_{\dot{x}}(\dot{x} - \dot{x}_d),$$
$$\ddot{y} = k_{\dot{y}}(\dot{y} - \dot{y}_d), \qquad (11)$$
$$\ddot{z} = k_{\dot{z}}\dot{z} + k_z(z - z_d),$$

where $k_{\dot{x}}$, $k_{\dot{y}}$, $k_{\dot{z}}$, and k_z are gains designed according to a required performance in terms of time responses. In order to meet this behavior the RHSs of (11) and (7) have to be forced to be equal by adjusting ϕ, θ, ψ, and θ_0 in a proper way. Since an explicit calculation is not feasible an optimization approach is suggested

at the end of which the corresponding ϕ, θ, ψ, and θ_0 are obtained (see also [4]). To do that, let both (7) and (11) be written in a compact way

$$\begin{pmatrix} \ddot{x} \\ \ddot{y} \\ \ddot{z} \end{pmatrix} = \tilde{f}(\phi, \theta, \psi, \theta_0), \qquad (12)$$

where the components of the vector function $\tilde{f}$ are given by the RHSs of (7) and

$$\tilde{u}(x, y, z) = \begin{pmatrix} k_{\dot{x}}(\dot{x} - \dot{x}_d) \\ k_{\dot{y}}(\dot{y} - \dot{y}_d) \\ k_{\dot{z}}\dot{z} + k_z(z - z_d) \end{pmatrix}. \qquad (13)$$

We calculate the vector $\xi = (\phi, \theta, \psi)^T$ and the scalar θ_0 by an optimization procedure for each time step using the quadratic cost function

$$V = \frac{1}{2}(\tilde{u} - \tilde{f}(\xi, \theta_0))^T(\tilde{u} - \tilde{f}(\xi, \theta_0)). \qquad (14)$$

Minimizing (14) is done by computing a change in V

$$\Delta V = -(\tilde{u} - \tilde{f}(\xi, \theta_0))^T(\tilde{B}_1\Delta\xi + \tilde{B}_2\Delta\theta_0) < 0, \quad (15)$$

where $\tilde{B}_1 = \frac{\partial \tilde{f}(\xi, \theta_0)}{\partial \xi} \in \Re^{3\times3}$ and $\tilde{B}_2 = \frac{\partial \tilde{f}(\xi, \theta_0)}{\partial \theta_0} \in \Re^{3\times1}$. This requires the computation of appropriate $\Delta\xi$ and $\Delta\theta_0$ that make $\Delta V < 0$. These are given as:

$$\Delta\xi = \begin{pmatrix} \Delta\phi \\ \Delta\theta \\ \Delta\psi \end{pmatrix} = \tilde{B}_1^T\alpha(\tilde{u} - \tilde{f}(\xi, \theta_0)), \qquad (16)$$

and

$$\Delta\theta_0 = \tilde{B}_2^T\beta(\tilde{u} - \tilde{f}(\xi, \theta_0)). \qquad (17)$$

In the above equations,

$$\alpha = \begin{pmatrix} \alpha_1 & 0 & 0 \\ 0 & \alpha_2 & 0 \\ 0 & 0 & \alpha_3 \end{pmatrix}; \quad \beta = \begin{pmatrix} \beta_1 & 0 & 0 \\ 0 & \beta_2 & 0 \\ 0 & 0 & \beta_3 \end{pmatrix} \quad (18)$$

define the widths of the optimization steps in each component, and $\alpha_i, \beta_i > 0, i = 1, 2, 3$. The optimiza-tion process stops either if the norm $\|\tilde{u} - \tilde{f}(\xi, \theta_0)\|$ falls below a defined threshold $\epsilon > 0$ or if the number i of optimization steps exceeds a certain limit. The proper choice of both the widths of the optimization steps and α_i, β_i is so far achieved by trial-and-error. We intend to use here a learning procedure in order to avoid the current tedious trial-and-error process.

3.1 Position Control

The position controller is designed in the same man-ner as the velocity/altitude controller. The only changes that have to be introduced to the design pro-cedure presented in the previous section are:

- Eq. (11) is replaced by:

$$\ddot{x} = k_x(x - x_d) + ki_x \int (x - x_d)dt + k_{\dot{x}}\dot{x},$$

$$\ddot{y} = k_y(y - y_d) + ki_y \int (y - y_d)dt + k_{\dot{y}}\dot{y},$$

$$\ddot{z} = k_{\dot{z}}\dot{z} + k_z(z - z_d),$$

where k_x, ki_x, $k_{\dot{x}}$, k_y, ki_y, $k_{\dot{y}}$, $k_{\dot{z}}$, and k_z are gains designed according to a required performance in terms of time responses.

- Eq. (13) is accordingly replaced by:

$$\tilde{u} = \begin{pmatrix} k_x(x - x_d) + ki_x \int (x - x_d)dt + k_{\dot{x}}\dot{x} \\ k_y(y - y_d) + ki_y \int (y - y_d)dt + k_{\dot{y}}\dot{y} \\ k_{\dot{z}}\dot{z} + k_z(z - z_d) \end{pmatrix}.$$

Figs. 10 and 11 illustrate the performance of the position controller.

4 Simulation Results

The numerical experiments are performed with the controllers designed in the previous sections and acting on the nonlinear model from Sect. 2.

The first experiment, depicted in Fig. 1, shows the results from set-point regulation around a desired low velocity combined with strong and weak wind action. Figure 2 shows results from the same experiment, but with high desired velocity.
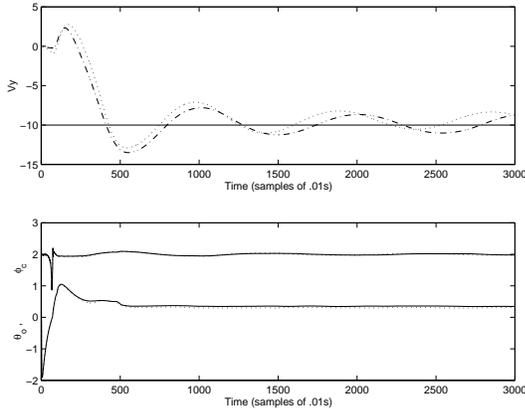
Figure 1: Upper-part: Low $\dot{y}$-velocity set-point regulation with strong and weak wind action, where desired –, strong wind -.– and weak ... wind. Lower-part: Control inputs for strong – and weak ... wind.

The second experiment, depicted in Fig. 3, shows the results from tracking a desired velocity trajectory with strong wind action. Figure 4 shows results from the same experiment, but with weak wind action.
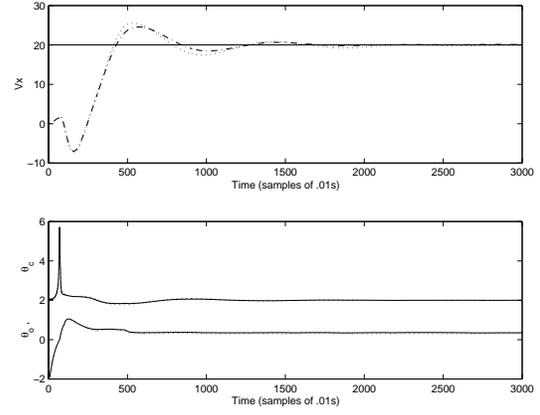

Figure 2: Upper-part: High $\dot{x}$-velocity set-point regulation with strong and weak wind action, desired –, strong -.– and weak ... wind. Lower-part: Control inputs for strong – and weak ... wind.
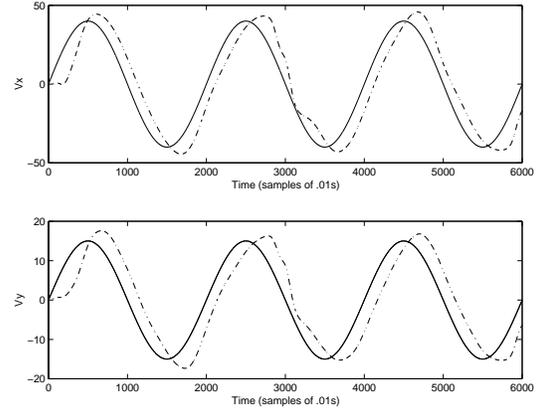

Figure 3: Velocity tracking with strong wind action, desired – and actual -.– .

The third experiment, see Fig. 5 and 6, shows results from velocity set-point changes for strong and weak wind action.

The fourth experiment shows results, see Fig. 7, from altitude set-point regulation – for strong and weak wind respectively. Figure 8 shows an altitude trajectory tracking.

The last experiments show results, see Figs. 9 and 10, from set-point position control with strong and weak wind action.

The diagrams show a time delay of approximately 2 sec. between the reference and the response for the altitude (z). The settling time for the attitude angles are respectively 3 sec., for the pitch and the roll, and 4 sec. for the yaw.
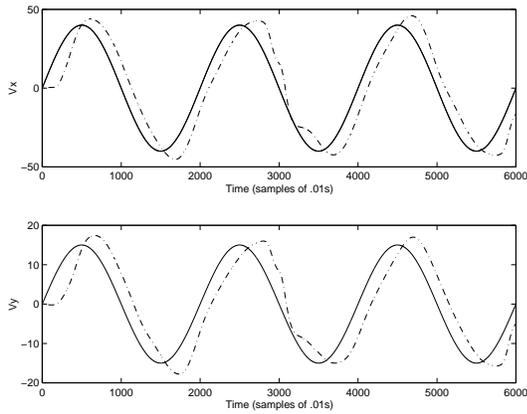
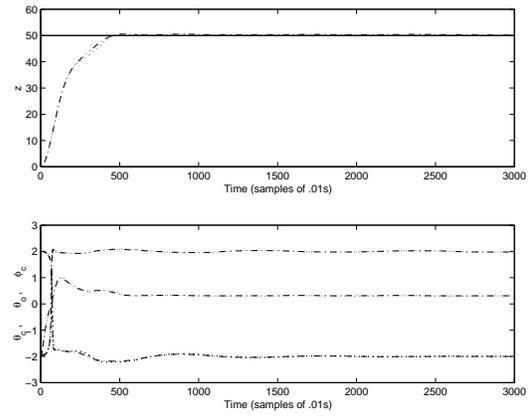Figure 4: Velocity tracking with weak wind action, desired − and actual -.− .

Figure 7: Altitude set-point regulation, desired − and actual -.− and control inputs.
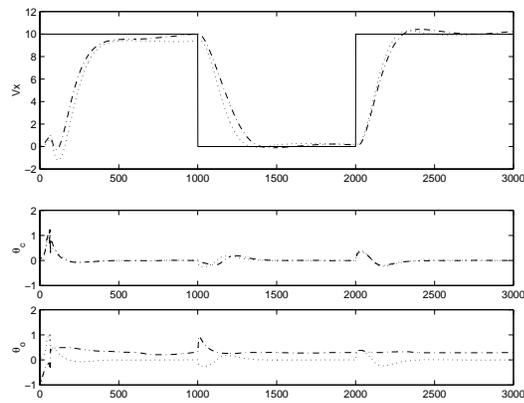

Figure 5: $\dot{x}$ set-point change, desired −, strong -.− and weak ... wind and control inputs.
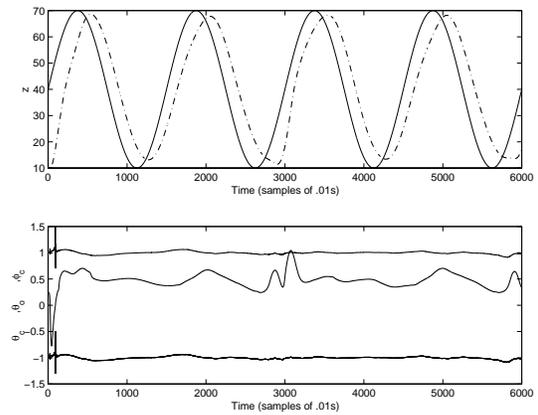

Figure 8: Altitude trajectory tracking, desired − and actual -.− and control inputs .
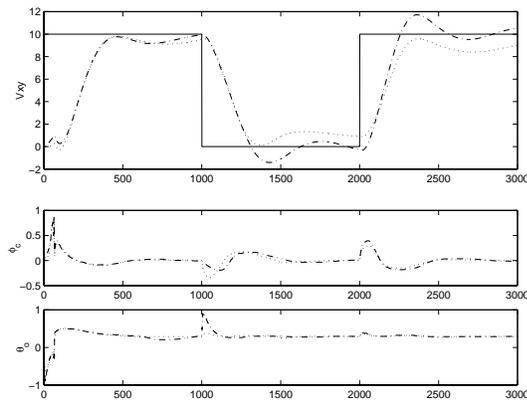

Figure 6: $\dot{y}$ set-point change, desired −, strong -.− and weak ... wind and control inputs.
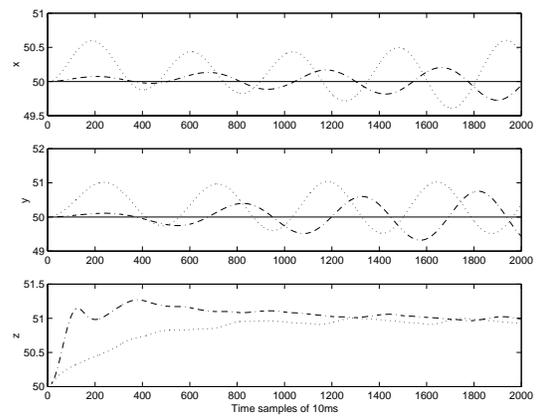

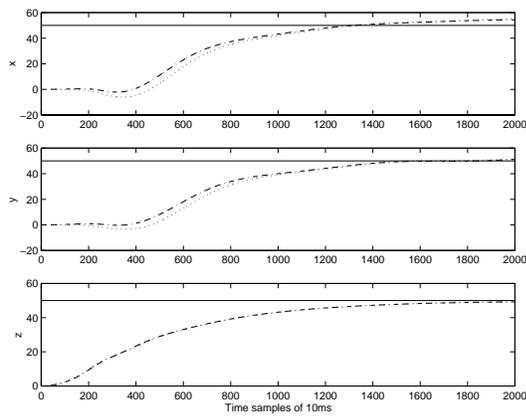Figure 9: Hovering with strong and weak wind, desired − , strong -.− and weak ... winds.

Figure 10: Set-point position control when the initial state is far from the set-point, desired − , strong -.− and weak ... winds.

5 Conclusions

This work has shown the applicability of our approach, using gradient descent optimization, to the velocity/altitude/position control of an unmanned helicopter. The performance of the controller when evaluated in simulation achieves stabilization of horizontal high-speed velocities, altitude, and position using attitude angles within much larger ranges than the ones currently available on the APID MK-III platform.

Future work will address the use of the approach presented here for the purpose of behavior-based helicopter control.

6 Acknowledgements

References

[1] T. J. Koo and S. Sastry, Output tracking control design of a helicopter model based on approximate linearization, Proceedings 37th IEEE Conference on Decision and Control, Tampa, Florida, USA, December 1998, pp. 3635–3640.

[2] J. E. Corban, A. J. Calise, and J. V. R. Prasad, Implementation of adaptive nonlinear control for flight test on an unmanned helicopter, Proceedings 37th IEEE Conference on Decision and Control, Tampa, Florida, USA, December 1998, pp. 3641–3646.

[3] B. Kadmiry, P. Bergsten, and D. Driankov, Autonomous helicopter control using fuzzy gain scheduling, submitted to ICRA 2001, Seoul, Korea, May 21–26, 2001.

[4] R.Palm, Ch. Stutz, and Th. Runkler, A control sequence generator for fuzzy gain schedulers, 39-th IEEE Conference on Decision and Control, Sydney, Australia, Dec. 12–15, 2000.